ELSEVIER

Nuclear Physics B 600 (2001) 39–61

NUCLEAR PHYSICS B

www.elsevier.nl/locate/npe

Neutralino phenomenology at LEP2 in supersymmetry with bilinear breaking of R-parity

A. Bartl [a], W. Porod [b], D. Restrepo [b], J. Romão [c], J.W.F. Valle [b]

[a] *Institut für Theor. Physik, Universität Wien, A-1090 Vienna, Austria*

[b] *Instituto de Física Corpuscular (IFIC), CSIC — Universidad de València, Edificio Institutos de Paterna, Apartado de Correos 22085, E-46071 València, Spain*

[c] *Departamento de Física, Instituto Superior Técnico, Av. Rovisco Pais 1, 1049-001 Lisboa, Portugal*

Received 18 July 2000; accepted 29 January 2001

Abstract

We discuss the phenomenology of the lightest neutralino in models where an effective bilinear term in the superpotential parametrizes the explicit breaking of R-parity. We consider supergravity scenarios where the lightest supersymmetric particle (LSP) is the lightest neutralino and which can be explored at LEP2. We present a detailed study of the LSP decay properties and general features of the corresponding signals expected at LEP2. We also contrast our model with gauge mediated supersymmetry breaking. © 2001 Elsevier Science B.V. All rights reserved.

1. Introduction

The search for supersymmetry (SUSY) plays an important role in the experimental programs of existing high energy colliders like LEP2, HERA and the Tevatron. It will play an even more important role at future colliders like LHC or a linear e^+e^- collider. So far most of the effort in searching for supersymmetric signatures has been confined to the framework of R-parity-conserving [1] realizations. Recent data on solar and atmospheric neutrinos strongly indicate the need for neutrino conversions [2,3]. Motivated by this there has been in the last few years a substantial interest in R-parity violating models [4]. The violation of R-parity could arise explicitly as a residual effect of some larger unified theory [5], or spontaneously, through nonzero vacuum expectation values (VEVs) for scalar neutrinos [6,7]. In the first case there is a large number of unknown parameters characterizing the superpotential of these models, so that for simplicity these effects are

E-mail address: porod@nac13.ific.uv.es (W. Porod).

0550-3213/01/$ – see front matter © 2001 Elsevier Science B.V. All rights reserved.
PII: S0550-3213(01)00042-6

usually studied assuming in an *ad hoc* way that only a few dominant terms break R-parity explicitly, usually only one.

We prefer theoretical scenarios which break R-parity only as a result of the properties of the vacuum [8]. There are two generic cases of spontaneous R-parity breaking models. In the first case lepton number is part of the gauge symmetry and there is a new gauge boson Z' which gets mass via the Higgs mechanism [9]. In this model the lightest SUSY particle (LSP) is in general a neutralino which decays, therefore, breaking R-parity. The LSP decays mostly to visible states such as

$$\tilde{\chi}_1^0 \to f\bar{f}\nu, \tag{1}$$

where f denotes a charged fermion. These decays are mediated by the Z-boson or by the exchange of scalars. In the second class of models there appears a physical massless Nambu–Goldstone boson, called majoron. The latter arises in $SU(2) \otimes U(1)$ models where the breaking of R-parity occurs spontaneously. In this case *the majoron is the LSP*, which is stable because it is massless (or nearly so). It leads to an additional invisible decay mode $\tilde{\chi}_1^0 \to \nu + J$, which is R-parity conserving since the majoron has a large R-odd singlet sneutrino component [10,11]. This decay is absent if lepton number is gauged, as the majoron is eaten up by a massive additional Z boson.

Although models with spontaneous R-parity breaking [9–11] usually contain additional fields not present in the MSSM in order to drive the violation of R-parity (expected to lie in the TeV range), they are characterized by much fewer parameters than models with explicit breaking of R-parity. Most phenomenological features of these models are reproduced by adding three explicit bilinear R-parity breaking terms to the MSSM superpotential [12]. This renders a systematic way to study R-parity breaking signals [13–15] and leads to effects that can be large enough to be experimentally observable, even in the case where neutrino masses are as small as indicated by the simplest interpretation of solar and atmospheric neutrino data [4]. Moreover, R-parity violating interactions follow a specific *pattern* which can be easily characterized. These features have been exploited in order to describe the R-parity violating signals expected for chargino production at LEP II [16].

Here we consider the phenomenology of the lightest neutralino in the simplest and well motivated class of models with an effective explicit R-parity breaking characterized by a single bilinear superpotential term [17]. Apart from the absence of the majoron-emitting $\tilde{\chi}_1^0$ decays (which are absent in majoron-less models with spontaneous breaking of R-parity) this bilinear model mimics all features of neutralino decay properties relevant for our analysis. For simplicity and for definiteness we consider supergravity scenarios where the lightest supersymmetric particle (LSP) is the lightest neutralino. We present a detailed study of the LSP decay properties and general features of the corresponding signals expected at LEP2. In the following we denote the minimal SUGRA scenario with conserved R-parity by mSUGRA. It is well known that in models with gauge mediated supersymmetry breaking (GMSB) the lightest neutralino decays [18,19], because the gravitino is the LSP. We, therefore, also discuss the possibilities to distinguish between GMSB and our R-parity breaking model.

2. The model

Here we will adopt a supersymmetric Lagrangian specified by the following superpotential

$$W = \varepsilon_{ab}\big[h_U^{ij}\widehat{Q}_i^a\widehat{U}_j\widehat{H}_2^b + h_D^{ij}\widehat{Q}_i^b\widehat{D}_j\widehat{H}_1^a + h_E^{ij}\hat{L}_i^b\widehat{R}_j\widehat{H}_1^a - \mu\widehat{H}_1^a\widehat{H}_2^b\big] + \varepsilon_{ab}\epsilon_i\hat{L}_i^a\widehat{H}_2^b, \tag{2}$$

where $i, j = 1, 2, 3$ are generation indices, $a, b = 1, 2$ are $SU(2)$ indices, and ε is a completely anti-symmetric 2×2 matrix, with $\varepsilon_{12} = 1$. The symbol "hat" over each letter indicates a superfield, with $\widehat{Q}_i$, $\hat{L}_i$, $\widehat{H}_1$, and $\widehat{H}_2$ being $SU(2)$ doublets with hypercharges $1/3$, -1, -1 and 1, respectively, and $\widehat{U}$, $\widehat{D}$, and $\widehat{R}$ being $SU(2)$ singlets with hypercharges $-4/3$, $2/3$ and 2, respectively. The couplings h_U, h_D, and h_E are 3×3 Yukawa matrices, and μ and ϵ_i are parameters with units of mass.

Supersymmetry breaking is parametrized by the standard set of soft supersymmetry breaking terms

$$\begin{aligned} V_{\text{soft}} = {} & M_Q^{ij2}\widetilde{Q}_i^{a*}\widetilde{Q}_j^a + M_U^{ij2}\widetilde{U}_i^*\widetilde{U}_j + M_D^{ij2}\widetilde{D}_i^*\widetilde{D}_j + M_L^{ij2}\tilde{L}_i^{a*}\tilde{L}_j^a + M_R^{ij2}\widetilde{R}_i^*\widetilde{R}_j \\ & + m_{H_1}^2 H_1^{a*}H_1^a + m_{H_2}^2 H_2^{a*}H_2^a \\ & - \left[\frac{1}{2}M_3\lambda_3\lambda_3 + \frac{1}{2}M\lambda_2\lambda_2 + \frac{1}{2}M'\lambda_1\lambda_1 + \text{h.c.}\right] \\ & + \varepsilon_{ab}\big[A_U^{ij}h_U^{ij}\widetilde{Q}_i^a\widetilde{U}_jH_2^b + A_D^{ij}h_D^{ij}\widetilde{Q}_i^b\widetilde{D}_jH_1^a + A_E^{ij}h_E^{ij}\tilde{L}_i^b\widetilde{R}_jH_1^a \\ & \qquad - B\mu H_1^aH_2^b + B_i\epsilon_i\tilde{L}_i^aH_2^b\big]. \end{aligned} \tag{3}$$

Note that, in the presence of soft supersymmetry breaking terms the bilinear terms ϵ_i cannot be rotated away, since the rotation, that eliminates it, reintroduces an R-parity violating trilinear term, as well as a sneutrino vacuum expectation value [17]. This happens even in the case where universal boundary conditions are adopted for the soft breaking terms at the unification scale, since universality will be effectively broken at the weak scale due to calculable renormalization effects. For definiteness and simplicity we will adopt this assumption throughout this paper.

Although for the discussion of flavour-changing processes, such as neutrino oscillations involving all three generations, it is important to consider the full three-generation structure of the model, for the following discussion of neutralino decay properties it will suffice to assume R-parity Violation (RPV) only in the third generation, as a first approximation. In this case we will omit the labels i, j in the superpotential and the soft breaking terms [17,20]

$$W = h_t\widehat{Q}_3\widehat{U}_3\widehat{H}_2 + h_b\widehat{Q}_3\widehat{D}_3\widehat{H}_1 + h_\tau\hat{L}_3\widehat{R}_3\widehat{H}_1 - \mu\widehat{H}_1\widehat{H}_2 + \epsilon_3\hat{L}_3\widehat{H}_2, \tag{4}$$

$$\begin{aligned} V_{\text{soft}} = {} & \varepsilon_{ab}\big[A_th_t\widetilde{Q}_3^a\widetilde{U}_3H_2^b + A_bh_b\widetilde{Q}_3^b\widetilde{D}_3H_1^a + A_\tau h_\tau\tilde{L}_3^b\widetilde{R}_3H_1^a \\ & - B\mu H_1^aH_2^b + B_3\epsilon_3\tilde{L}_3^aH_2^b\big] + \text{mass terms}. \end{aligned} \tag{5}$$

This amounts to neglecting the $\not{R}_p$ effects in the two first families.

The bilinear terms in Eqs. (4) and (5) lead to a mixing between the charginos and the τ-lepton which is described by the mass matrix

$$\mathbf{M}_{\mathrm{C}} = \begin{bmatrix} M_2 & \frac{1}{\sqrt{2}} g v_2 & 0 \\ \frac{1}{\sqrt{2}} g v_1 & \mu & -\frac{1}{\sqrt{2}} h_\tau v_3 \\ \frac{1}{\sqrt{2}} g v_3 & -\epsilon_3 & \frac{1}{\sqrt{2}} h_\tau v_1 \end{bmatrix}, \tag{6}$$

where v_1, v_2, and v_3 are the vevs of H_1^0, H_2^0, and $\tilde{\nu}_\tau$, respectively. As in the MSSM, the chargino mass matrix is diagonalized by two rotation matrices $\mathbf{U}$ and $\mathbf{V}$

$$\mathbf{U}^* \mathbf{M}_{\mathrm{C}} \mathbf{V}^{-1} = \begin{bmatrix} m_{\tilde{\chi}_1^\pm} & 0 & 0 \\ 0 & m_{\tilde{\chi}_2^\pm} & 0 \\ 0 & 0 & m_\tau \end{bmatrix}. \tag{7}$$

The lightest eigenstate of this mass matrix must be the tau lepton ($\tau^\pm$) and so the mass is constrained to be 1.7771 GeV. As explained in [21], the tau Yukawa coupling becomes a function of the SUSY parameters appearing in the mass matrix.

The neutralino mass matrix is given by:

$$\mathbf{M}_{\mathrm{N}} = \begin{bmatrix} M_1 & 0 & -g_1 v_1 & g_1 v_2 & -g_1 v_3 \\ 0 & M_2 & g_2 v_1 & -g_2 v_2 & g_2 v_3 \\ -g_1 v_1 & g_2 v_1 & 0 & -\mu & 0 \\ g_1 v_2 & -g_2 v_2 & -\mu & 0 & \epsilon_3 \\ -g_1 v_3 & g_2 v_3 & 0 & \epsilon_3 & 0 \end{bmatrix}, \tag{8}$$

where $g_1 = g'/2$ and $g_2 = g/2$ denote gauge couplings. This matrix is diagonalised by a 5×5 unitary matrix N,

$$\chi_i^0 = N_{ij} \psi_j^0, \tag{9}$$

where $\psi_j^0 = (-i\widetilde{B}, -i\widetilde{W}_3, \widetilde{H}_d, \widetilde{H}_u, \nu_\tau)$.

The up squark mass matrix is given by

$$M_{\tilde{u}}^2 = \begin{bmatrix} M_Q^2 + \frac{1}{2} v_2^2 {h_u}^2 + \Delta_{UL} & \frac{h_u}{\sqrt{2}} (v_2 A_u - \mu v_1 + \epsilon_3 v_3) \\ \frac{h_u}{\sqrt{2}} (v_2 A_u - \mu v_1 + \epsilon_3 v_3) & M_U^2 + \frac{1}{2} v_2^2 {h_u}^2 + \Delta_{UR} \end{bmatrix}, \tag{10}$$

and the down squark mass matrix by

$$M_{\tilde{d}}^2 = \begin{bmatrix} M_Q^2 + \frac{1}{2} v_1^2 {h_d}^2 + \Delta_{DL} & \frac{h_d}{\sqrt{2}} (v_1 A_d - \mu v_2) \\ \frac{h_d}{\sqrt{2}} (v_1 A_d - \mu v_2) & M_D^2 + \frac{1}{2} v_1^2 {h_d}^2 + \Delta_{DR} \end{bmatrix}, \tag{11}$$

with $\Delta_{UL} = \frac{1}{8}(g^2 - \frac{1}{3} g'^2)(v_1^2 - v_2^2 + v_3^2)$, $\Delta_{DL} = \frac{1}{8}(-g^2 - \frac{1}{3} g'^2)(v_1^2 - v_2^2 + v_3^2)$, $\Delta_{UR} = \frac{1}{6} g'^2 (v_1^2 - v_2^2 + v_3^2)$, and $\Delta_{DR} = -\frac{1}{12} g'^2 (v_1^2 - v_2^2 + v_3^2)$. The sum of the v_i^2 is given by $m_W^2 = g^2 (v_1^2 + v_2^2 + v_3^2)/2$. The mass eigenstates are given by $\tilde{q}_1 = \tilde{q}_L \cos\theta_{\tilde{q}} + \tilde{q}_R \sin\theta_{\tilde{q}}$ and $\tilde{q}_2 = \tilde{q}_R \cos\theta_{\tilde{q}} - \tilde{q}_L \sin\theta_{\tilde{q}}$. The sfermion mixing angle is given by

$$\cos\theta_{\tilde{q}} = \frac{-M_{\tilde{q}_{LR}}^2}{\sqrt{\left(M_{\tilde{q}_{LL}}^2 - m_{\tilde{q}_1}^2\right)^2 + \left(M_{\tilde{q}_{LR}}^2\right)^2}},$$

$$\sin\theta_{\tilde{q}} = \frac{M_{\tilde{q}_{LL}}^2 - m_{\tilde{q}_1}^2}{\sqrt{\left(M_{\tilde{q}_{LL}}^2 - m_{\tilde{q}_1}^2\right)^2 + \left(M_{\tilde{q}_{LR}}^2\right)^2}}. \tag{12}$$

Here $M_{\tilde{q}_{ij}}^2$ are the corresponding entries of the mass matrices in Eqs. (10) and (11).

In addition the charged Higgs bosons mix with charged sleptons and the real (imaginary) parts of the sneutrino mix the scalar (pseudoscalar) Higgs bosons. The formulas can be found in [21,22] and are reproduced, for completeness, in Appendix A. The corresponding mass eigenstates are denoted by S_i^+ for the charged scalars, S_j^0 for the neutral scalars, and P_k^0 for the pseudoscalars.

3. Numerical results

In this section we present numerical predictions for the lightest and second lightest neutralino production cross sections in e^+e^- collisions, namely, $e^+e^- \to \tilde{\chi}_1^0\tilde{\chi}_1^0$, $\tilde{\chi}_1^0\tilde{\chi}_2^0$. Moreover, we will characterize in detail all branching ratios for the lightest neutralino decays, which violate R-parity.

The relevant parameters include the $\not{R}_p$ parameters and the standard mSUGRA parameters $M_{1/2}$, m_0, $\tan\beta$, where $M_{1/2}$ is the common gaugino mass, m_0 the common scalar mass, and $\tan\beta = v_2/v_1$ is the ratio of the vacuum expectation values of the Higgs fields. The absolute value of μ is fixed by radiative breaking of electroweak symmetry. We take μ positive to be in agreement with the $b \to s\gamma$ decay [23]. As representative values of $\tan\beta$ we take $\tan\beta = 3$ and 50. It is a feature of models with purely spontaneous breaking of R-parity that neutrinos acquire a mass only due to the violation of R-parity [6,7,24]. This feature also applies to models characterized by purely bilinear breaking of R-parity, like our reference model characterized by Eqs. (4) and (5). As a result the $\not{R}_p$ violating parameters are directly related with m_{ν_3}, the mass of the neutrino ν_3, which is generated due to the mixing implicit in Eq. (8).

3.1. Neutralino production

While the violation of R-parity would allow for the single production of supersymmetric particles [13], for the assumed values of the $\not{R}_p$ violation parameters indicated by the simplest interpretation of solar and atmospheric neutrino data [2,3], these cross sections are typically too small to be observable. As a result neutralino production at LEP2 in our model typically occurs in pairs with essentially the same cross sections as in the mSUGRA case. In Fig. 1(a) and (b) we show the maximum and minimum attainable values for the $e^+e^- \to \tilde{\chi}_1^0\tilde{\chi}_1^0$ and $e^+e^- \to \tilde{\chi}_1^0\tilde{\chi}_2^0$ production cross sections as a function of $m_{\tilde{\chi}_1^0}$ at $\sqrt{s} = 205$ GeV. We compare the cases $\tan\beta = 3$ and $\tan\beta = 50$, varying $M_{1/2}$ between 90 GeV and 260 GeV and m_0 between 50 GeV and 500 GeV. One can see that, indeed, these results are identical to those obtained in the mSUGRA. The $\tilde{\chi}_1^0\tilde{\chi}_1^0$ production cross section can reach approximately 1 pb. In our calculation we have used the formula as given in [25] and, in addition, we have included initial state radiation (ISR) using the formula given in [26]. Note that $\tilde{e}_L$ and $\tilde{e}_R$ are exchanged in the t- and u-channel implying that a large fraction of the neutralinos will be produced in the forward and backward directions.

In order to show more explicitly the dependence of the cross sections on the parameters m_0 and $M_{1/2}$ we plot in Fig. 2(a) and (b) the contour lines of $\sigma(e^+e^- \to \tilde{\chi}_1^0\tilde{\chi}_1^0)$ in the

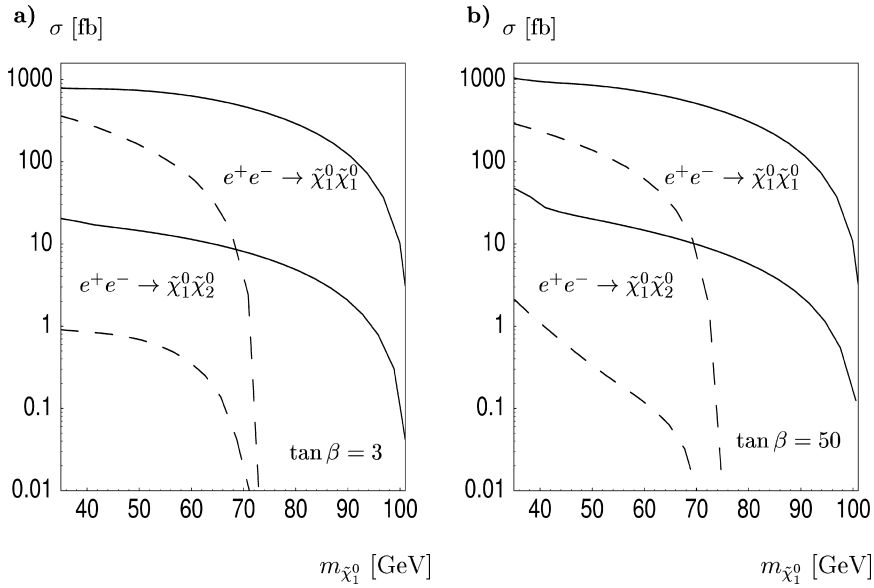

Fig. 1. Maximum and minimum attainable values for the $e^+e^- \to \tilde{\chi}_1^0\tilde{\chi}_1^0$ (full lines) and $e^+e^- \to \tilde{\chi}_1^0\tilde{\chi}_2^0$ (dashed lines) production cross sections in fb as a function of $m_{\tilde{\chi}_1^0}$ for $\sqrt{s} = 205$ GeV, 50 GeV $< m_0 <$ 500 GeV, 90 GeV $< M_{1/2} <$ 270 GeV, (a) $\tan\beta = 3$, and (b) $\tan\beta = 50$. ISR corrections are included.

m_0-$M_{1/2}$ plane at $\sqrt{s} = 205$ GeV for $\tan\beta = 3$ and $\tan\beta = 50$. The contour lines for $\sigma(e^+e^- \to \tilde{\chi}_1^0\tilde{\chi}_2^0)$ are given in Fig. 2(c) and (d).

3.2. Neutralino decay length

If unprotected by the ad hoc assumption of R-parity conservation the LSP will decay as a result of gauge boson, squark, slepton and Higgs boson exchanges. The relevant contributions to these decays are given in Table 1. The Feynman diagrams for the decays not involving taus, i.e., $\tilde{\chi}_1^0 \to \nu_3 f \bar{f}$ ($f = e, \nu_e, \mu, \nu_\mu, u, d, c, s, b$) are shown explicitly in Fig. 3.

For the observability of the R-parity violating effects it is crucial that with this choice of parameters the LSP will decay most of the time inside the detector. The neutralino decay path expected at LEP2 depends crucially on the values of $\not{R}_p$ violating parameters or, equivalently, on the value of the heaviest neutrino mass, m_{ν_3}. We fix the value of m_{ν_3} as indicated by the analyses of the atmospheric neutrino data [3]. It is important to note that, as explained in [4], due to the projective nature of the neutrino mass matrix [7], only one of the three neutrinos picks up a mass in tree approximation. This means that, neglecting radiative corrections which give small masses to the first two neutrinos in order to account for the solar neutrino data, the neutralino decay length scale is set mainly by the tree-level value of m_{ν_3}. In Ref. [4] we have explicitly shown that this is a good approximation for most points in parameter space.

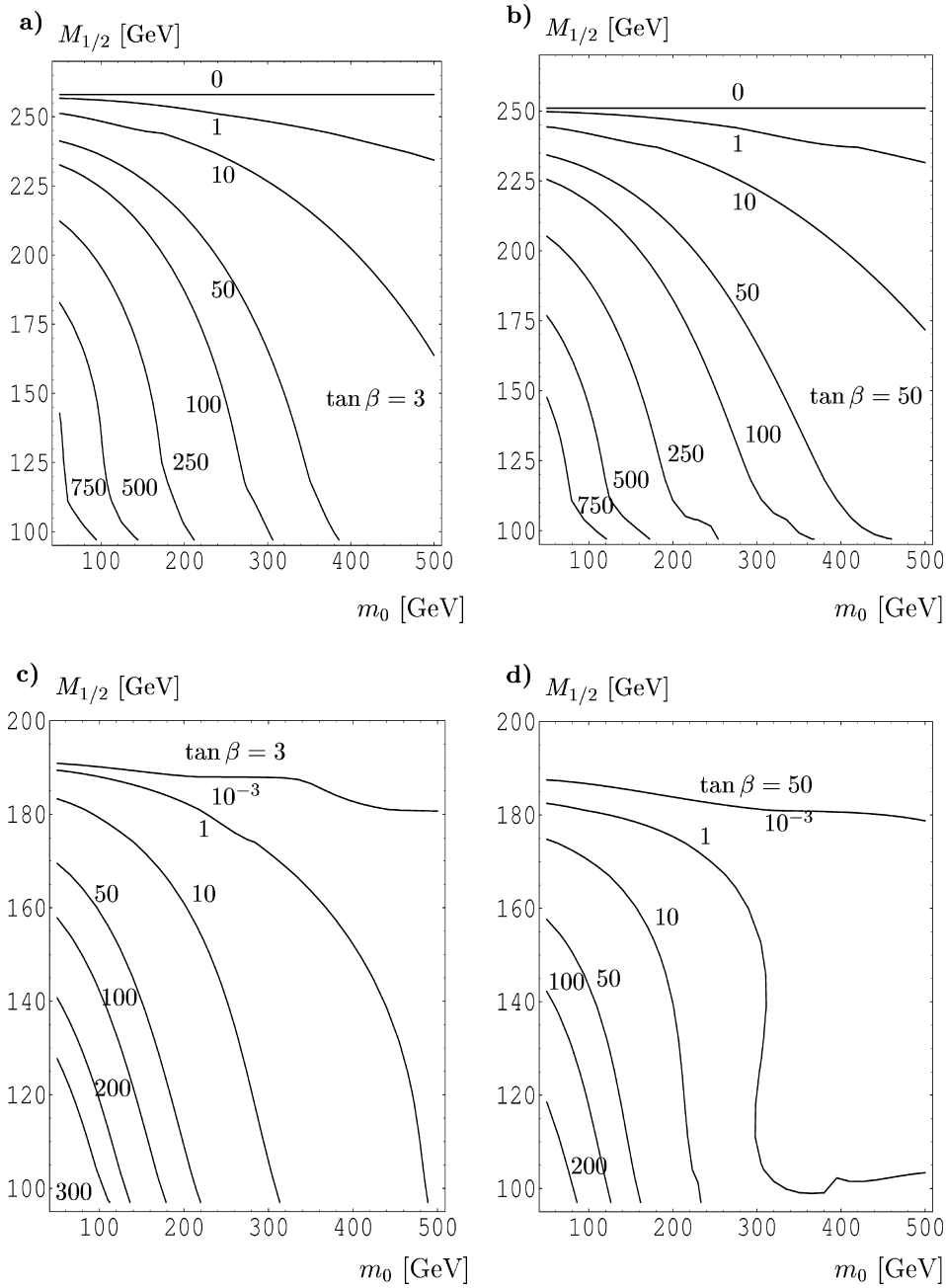

Fig. 2. Contour lines of the production cross sections in fb, in the m_0–$M_{1/2}$ plane for $\sqrt{s} = 205$ GeV, (a) $e^+e^- \to \tilde{\chi}_1^0\tilde{\chi}_1^0$, $\tan\beta = 3$, (b) $e^+e^- \to \tilde{\chi}_1^0\tilde{\chi}_1^0$, $\tan\beta = 50$, (c) $e^+e^- \to \tilde{\chi}_1^0\tilde{\chi}_2^0$, $\tan\beta = 3$, and (d) $e^+e^- \to \tilde{\chi}_1^0\tilde{\chi}_2^0$, $\tan\beta = 50$. ISR corrections are included.

Table 1
Contributions involved in the lightest neutralino 3-body decay modes. The s-, t-, and u-channels are defined by: $s = (p_1 - p_2)^2$, $t = (p_1 - p_3)^2$, and $u = (p_1 - p_4)^2$. See also Fig. 3

Decay mode	Exchanged particle	Channel
$\tilde{\chi}_1^0 \to 3\nu_3$	Z, S_i^0, P_j^0	s
	Z, S_i^0, P_j^0	t
	Z, S_i^0, P_j^0	u
$\tilde{\chi}_1^0 \to \nu_3 \nu_l \bar{\nu}_l$ $(l = e, \mu)$	Z	s
	$\bar{\tilde{\nu}}_l$	t
	$\tilde{\nu}_l$	u
$\tilde{\chi}_1^0 \to \nu_3 f \bar{f}$ $(f = e, \mu, u, d, s, c, b)$	Z, S_i^0, P_j^0	s
	$\bar{\tilde{f}}_{1,2}$	t
	$\tilde{f}_{1,2}$	u
$\tilde{\chi}_1^0 \to \nu_3 \tau^+ \tau^-$	Z, S_i^0, P_j^0	s
	W^-, S_k^-	t
	W^+, S_k^+	u
$\tilde{\chi}_1^0 \to \nu_l \tau^\pm l^\mp$ $(l = e, \mu)$	$W^\pm, S_k^\pm$	s
	$\bar{\tilde{l}}_{1,2}$	t
	$\tilde{\nu}_l$	u
$\tilde{\chi}_1^0 \to \tau q \bar{q}'$ $(q = u, c, q' = d, s)$	$W^\pm, S_k^\pm$	s
	$\bar{\tilde{q}}'_{1,2}$	t
	$\tilde{q}_{1,2}$	u

In Fig. 4 we plot the $\tilde{\chi}_1^0$ decay length in cm expected at LEP2 for $\sqrt{s} = 205$ GeV. Here and later on we consider the neutralinos stemming from the process $e^+e^- \to \tilde{\chi}_1^0 \tilde{\chi}_1^0$ when discussing the decay length. In Fig. 4(a) we plot the $\tilde{\chi}_1^0$ decay length in cm as a function of neutrino mass m_{ν_3}, for different $m_{\tilde{\chi}_1^0}$ between 60 and 90 GeV, with $m_0 = 100$ GeV, and $\tan\beta = 3$. As can be seen the expected neutralino decay length is typically such that the decays occur inside the detector, leading to a drastic modification of the mSUGRA signals. An equivalent way of presenting the neutralino decay path at LEP2 is displayed in Fig. 4(b), which gives the decay length of $\tilde{\chi}_1^0$ as a function of $m_{\tilde{\chi}_1^0}$ for $m_{\nu_3} = 0.01$, 0.1, and 1 eV. Finally, we show the dependence of the neutralino decay path on the supergravity parameters fixing the magnitude of $\not{R}_p$ violating parameters or, equivalently, the magnitude of the heaviest neutrino mass, m_{ν_3}. In Fig. 5(a) and (b) we plot the contour lines of the decay length of $\tilde{\chi}_1^0$ in the m_0–$M_{1/2}$ plane for $m_{\nu_3} = 0.06$ eV, $\tan\beta = 3$ and 50. Note that the decay length is short enough that it may happen inside typical high energy collider detectors even for the small neutrino mass values ~ 0.06 eV indicated by the

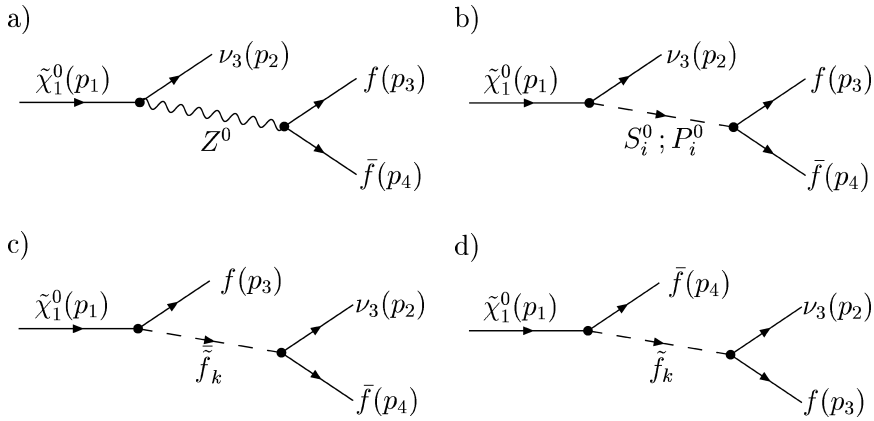

Fig. 3. Feynman graphs for the decay $\tilde{\chi}_1^0 \to \nu_3 f \bar{f}$ where $f \neq \tau$.

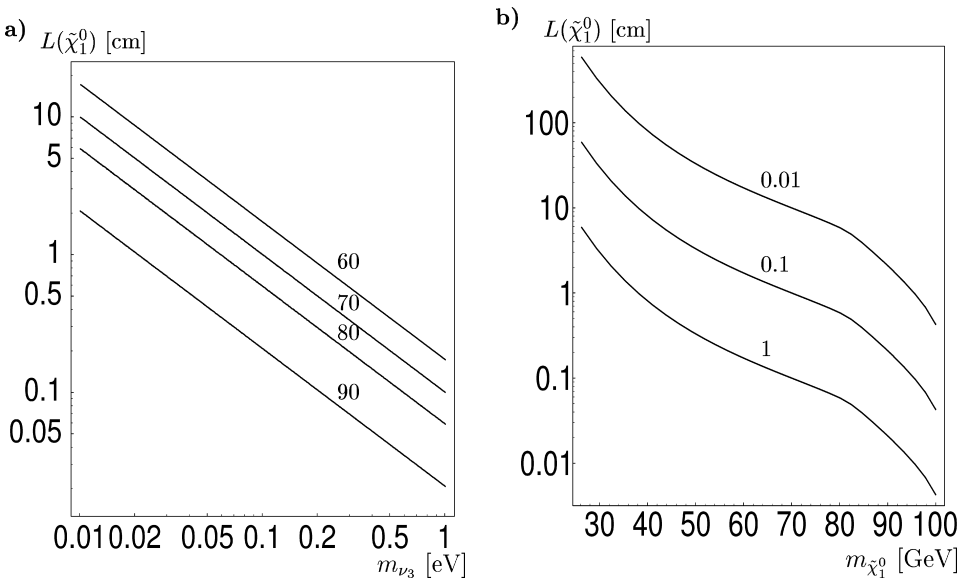

Fig. 4. Decay length of the lightest neutralino in cm for $\sqrt{s} = 205$ GeV, (a) as a function of m_{ν_3} for $m_{\tilde{\chi}_1^0} = 60, 70, 80$, and 90 GeV, (b) as a function of $m_{\tilde{\chi}_1^0}$ for $m_{\nu_3} = 0.01, 0.1$, and 1 eV.

atmospheric neutrino data [3]. For large values of $\tan\beta$ the total decay width increases and, correspondingly, the decay path decreases due to the tau Yukawa coupling and the bottom Yukawa coupling.

3.3. Neutralino branching ratios

As discussed in the beginning of this section, the lightest neutralino $\tilde{\chi}_1^0$ will typically decay in the detector. In the following we present our results for the branching ratios of all

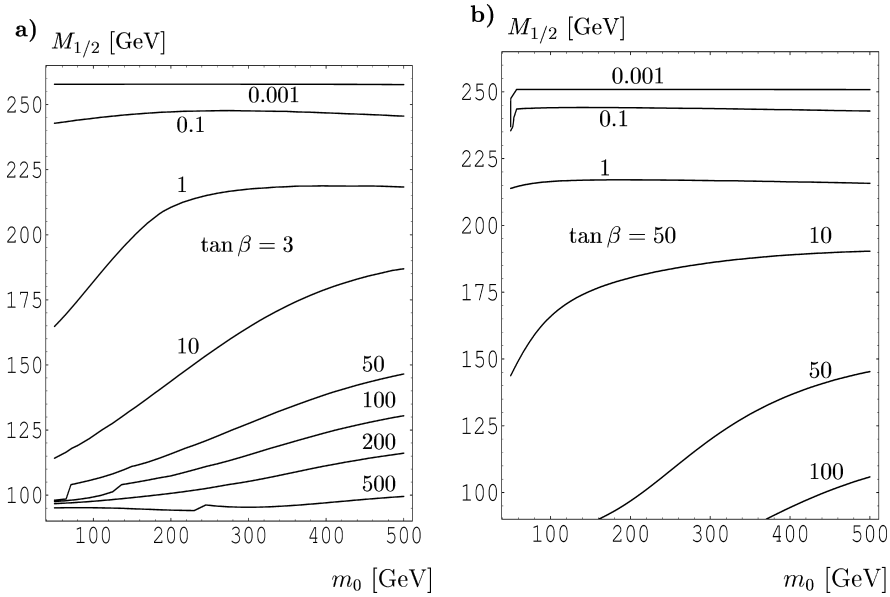

Fig. 5. Decay length of the lightest neutralino in cm in the m_0–$M_{1/2}$ plane for $\sqrt{s} = 205$ GeV, (a) $\tan\beta = 3$, and (b) $\tan\beta = 50$. The R-parity violating parameters are fixed such that $m_{\nu_3} = 0.06$ GeV.

R-parity violating 3-body decay of $\tilde{\chi}_1^0$, and of the radiative decay $\tilde{\chi}_1^0 \to \nu_3\gamma$. The Feynman diagrams for the decays $\tilde{\chi}_1^0 \to \nu_3 f \bar{f}$ ($f = e, \nu_e, \mu, \nu_\mu, u, d, c, s, b$) are shown in Fig. 3. For this class of decays we have Z^0, P_i^0, and S_j^0 exchange in the direct channel (Fig. 3(a) and (b)) and $\tilde{f}$ exchange in the crossed channels (Fig. 3(c) and (d)). In particular in the case $f = b$ the P_i^0 and S_j^0 exchange contributions are significant. This is quite analogous to the results found in [27] for $\tilde{\chi}_2^0 \to \tilde{\chi}_1^0 f \bar{f}$ decays. The particles exchanged in the s-, t-, and u-channel for the decays $\tilde{\chi}_1^0 \to \tau^\pm l^\mp \nu_l$ ($l = e, \mu$), $\tilde{\chi}_1^0 \to \tau^\pm q \bar{q}'$ ($q, q' = u, d, s, c$), $\tilde{\chi}_1^0 \to \tau^- \tau^+ \nu_l$, and $\tilde{\chi}_1^0 \to 3\nu_3$ are given in Table 1.

In the calculations we have included all mixing effects, in particular the standard MSSM $\tilde{f}_L$–$\tilde{f}_R$ mixing effects and those induced by the bilinear R-parity violating terms, i.e., $\mathrm{Re}(\tilde{\nu}_\tau) - h^0 - H^0$, $\mathrm{Im}(\tilde{\nu}_3) - A^0 - G^0$, [28], $\tilde{\tau}_{L,R}^\pm - H^\pm - G^\pm$ [21], $\nu_\tau - \tilde{\chi}_i^0$ [24], and $\tau - \tilde{\chi}_j^-$ mixings [13]. These mixing effects are particularly important in the calculations of the various R-parity violating decay rates of $\tilde{\chi}_1^0$, which are discussed below.

In the following plots Figs. 6–13 we show contour lines in the m_0–$M_{1/2}$ plane for the branching ratios in % of the various $\tilde{\chi}_1^0$ decays, in (a) for $\tan\beta = 3$ and in (b) for $\tan\beta = 50$. We have fixed the mass of the heaviest neutrino to $m_{\nu_3} = 0.06$ eV [3]. It turns out, that in the range 10^{-2} eV $\leqslant m_{\nu_3} \leqslant 1$ keV all the $\tilde{\chi}_1^0$ decay branching ratios are rather insensitive to the actual value of m_{ν_3}. This is an important feature of our supergravity-type R-parity violating model. It is a consequence of the fact that, as a result of the universal supergravity boundary conditions on the soft breaking terms, all R-parity violating couplings are proportional to a unique common parameter which may be taken as ϵ_3/μ. For a more detailed discussion

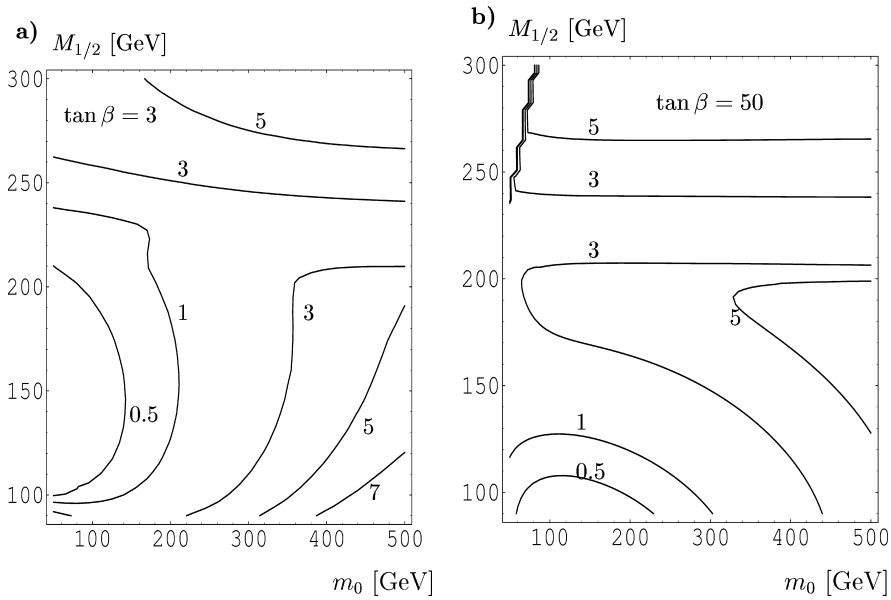

Fig. 6. Branching ratios for $\tilde{\chi}_1^0 \to 3\nu$ in % in the m_0–$M_{1/2}$ plane for (a) $\tan\beta = 3$, and (b) $\tan\beta = 50$. The R-parity violating parameters are fixed such that $m_{\nu_3} = 0.06$ GeV.

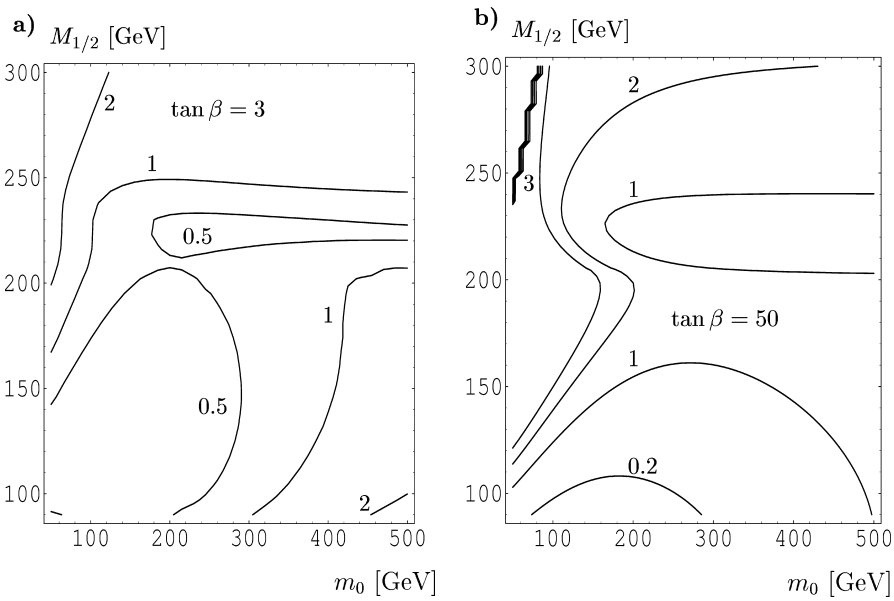

Fig. 7. Branching ratios for $\tilde{\chi}_1^0 \to \nu_3 l^+ l^-$ in % in the m_0–$M_{1/2}$ plane for (a) $\tan\beta = 3$, and (b) $\tan\beta = 50$. Here l is the sum of e and μ. The R-parity violating parameters are fixed such that $m_{\nu_3} = 0.06$ GeV.

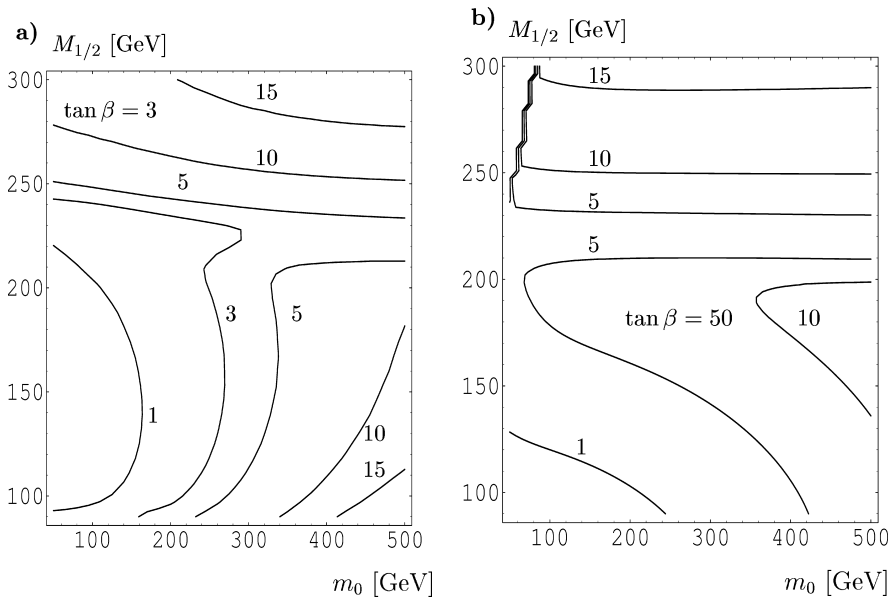

Fig. 8. Branching ratios for $\tilde{\chi}_1^0 \to \nu_3 q\bar{q}$ in % in the m_0–$M_{1/2}$ plane for (a) $\tan\beta = 3$, and (b) $\tan\beta = 50$. Here q is the sum over u, d, s, and c. The R-parity violating parameters are fixed such that $m_{\nu_3} = 0.06$ GeV.

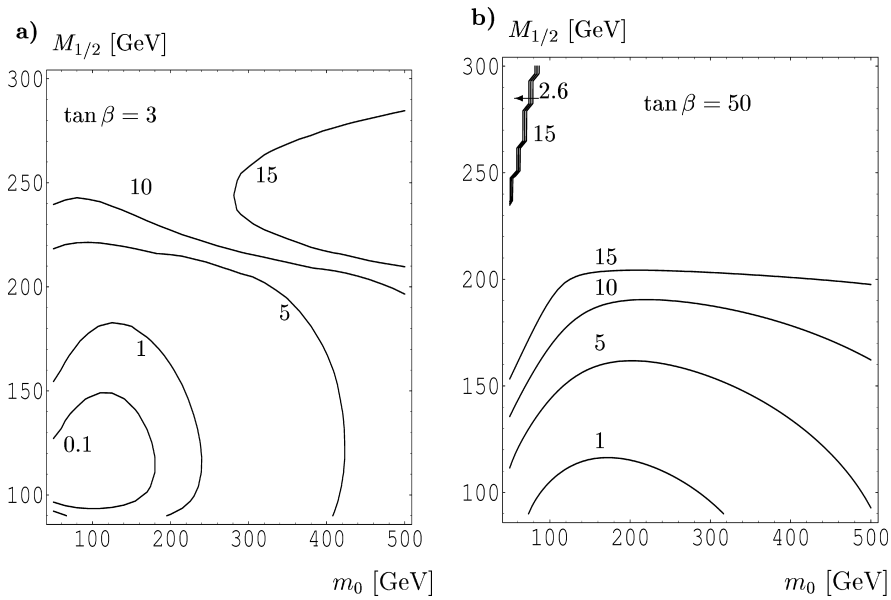

Fig. 9. Branching ratios for $\tilde{\chi}_1^0 \to \nu_l \tau^{\pm} l^{\mp}$ in % in the m_0–$M_{1/2}$ plane for (a) $\tan\beta = 3$, and (b) $\tan\beta = 50$. Here l is the sum of e and μ. The R-parity violating parameters are fixed such that $m_{\nu_3} = 0.06$ GeV.

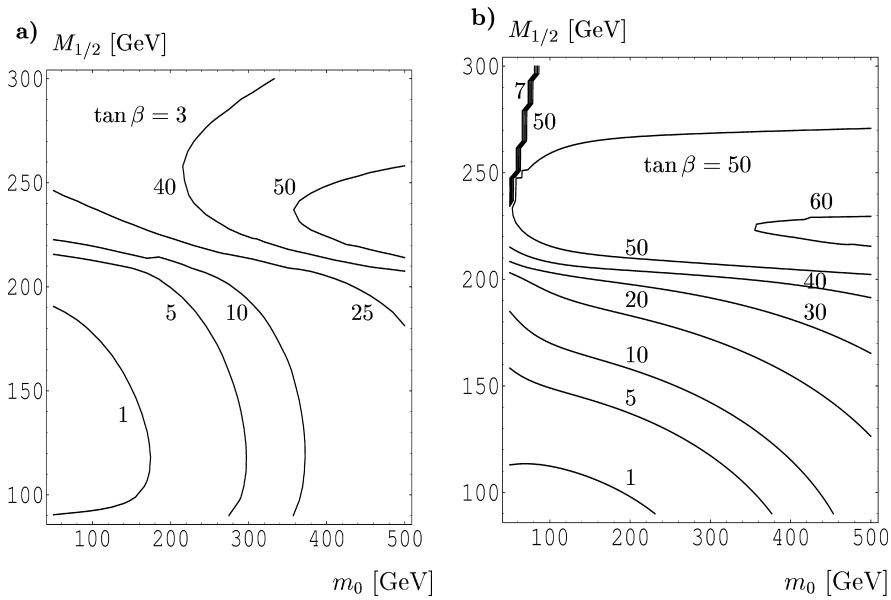

Fig. 10. Branching ratios for $\tilde{\chi}_1^0 \to \tau^{\pm} q\bar{q}'$ in % in the m_0–$M_{1/2}$ plane for (a) $\tan\beta = 3$, and (b) $\tan\beta = 50$. Here q is the sum over u, d, s, and c. The R-parity violating parameters are fixed such that $m_{\nu_3} = 0.06$ GeV.

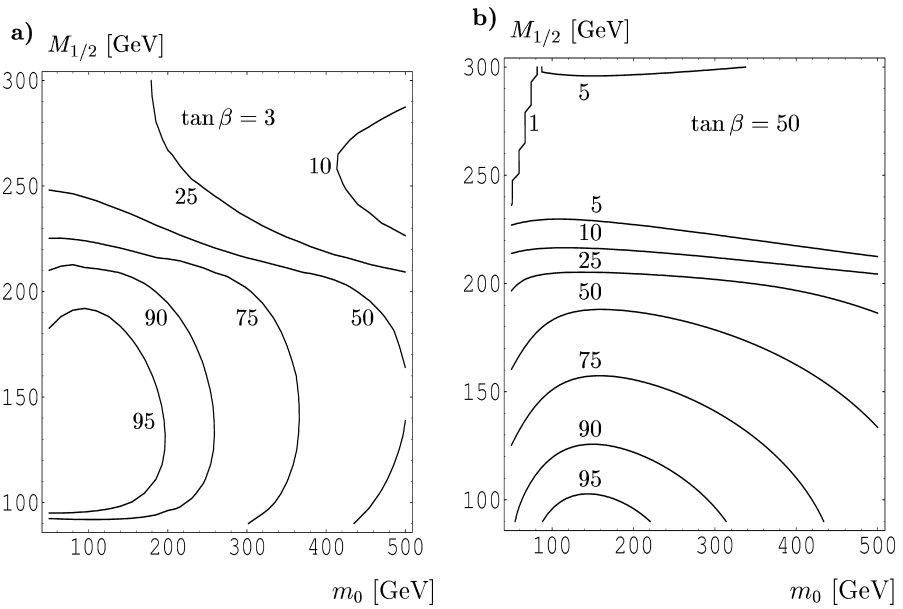

Fig. 11. Branching ratios for $\tilde{\chi}_1^0 \to \nu_3 b\bar{b}$ in % in the m_0–$M_{1/2}$ plane for (a) $\tan\beta = 3$, and (b) $\tan\beta = 50$. The R-parity violating parameters are fixed such that $m_{\nu_3} = 0.06$ GeV.

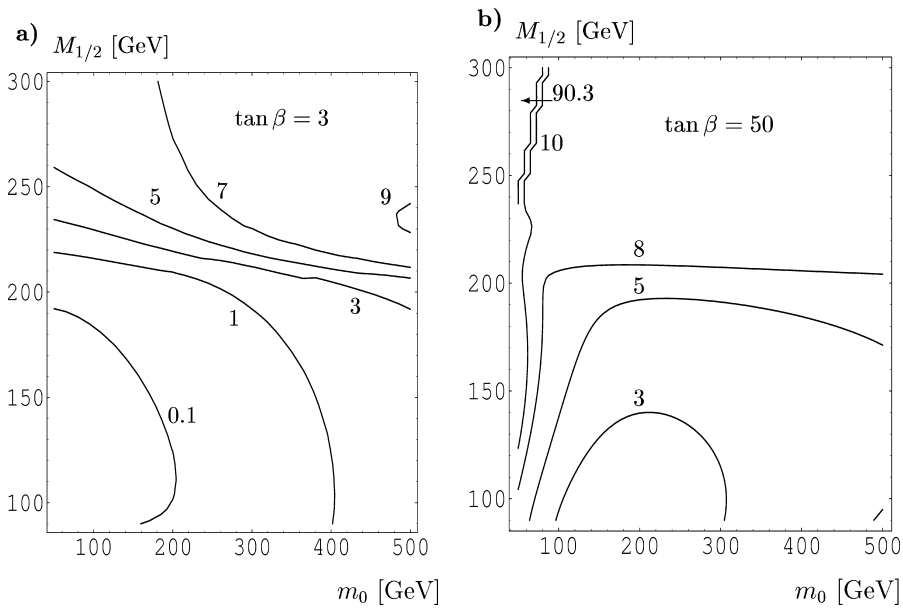

Fig. 12. Branching ratios for $\tilde{\chi}_1^0 \to \nu_3\tau^+\tau^-$ in % in the m_0–$M_{1/2}$ plane for (a) $\tan\beta = 3$, and (b) $\tan\beta = 50$. The R-parity violating parameters are fixed such that $m_{\nu_3} = 0.06$ GeV.

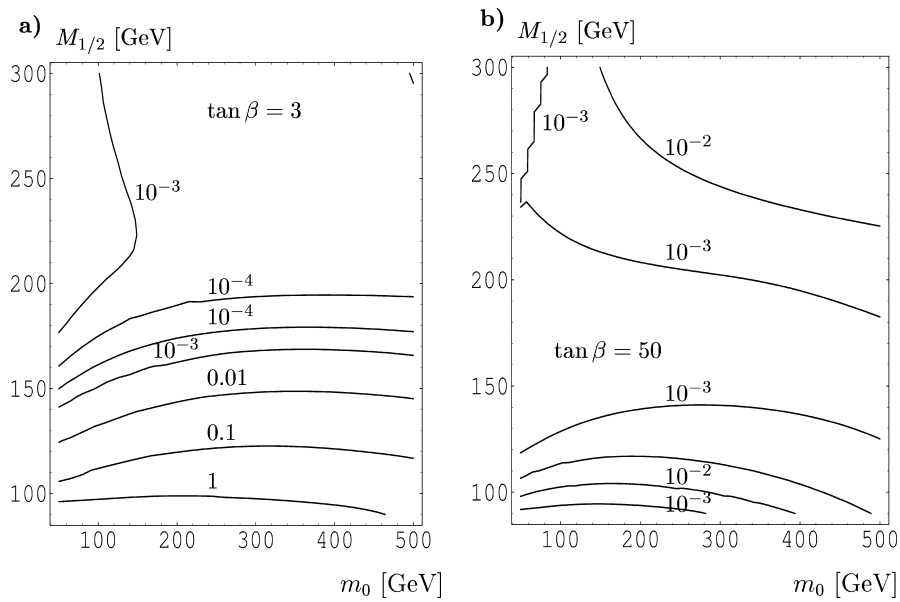

Fig. 13. Branching ratios for $\tilde{\chi}_1^0 \to \nu_3\gamma$ in % in the m_0–$M_{1/2}$ plane for (a) $\tan\beta = 3$, and (b) $\tan\beta = 50$. The R-parity violating parameters are fixed such that $m_{\nu_3} = 0.06$ GeV.

on this proportionality the reader is referred to Ref. [4]. Also note that for $M_{1/2} \gtrsim 220$ GeV the neutralino mass becomes larger than m_W and m_Z so that $\tilde{\chi}_1^0$ decays into real W and Z are possible. The effects of these real decays can be seen for $M_{1/2} \gtrsim 220$ GeV in most of the following plots. For the large $\tan\beta$ case ($\tan\beta = 50$) and $M_{1/2} \gg M_0$ the mass of the lighter charged boson $S_1^{\pm}$ is smaller than $m_{\tilde{\chi}_1^0}$ (upper left corner of Figs. 6(b)–13(b)). In this region of the parameter space the two 2-body decays $\tilde{\chi}_1^0 \to W^{\pm}\tau^{\mp}$ and $\tilde{\chi}_1^0 \to S_1^{\pm}\tau^{\mp}$ compete. The first one is R-parity violating, but has more phase space than the second one which is R-parity conserving, since $S_1^{\pm}$ is mainly a stau. For this reason, the most import final state is $\tau^+\tau^-\nu_3$, followed by $\tau^{\pm}q\bar{q}'$ and $\tau^{\pm}l^{\mp}\nu_i$ ($l = e, \mu$) as shown in Figs. 12, 10 and 9, respectively. All other final states have nearly vanishing branching ratios in this corner of the parameter space.

Fig. 6(a) and (b) exhibit the contour lines for the branching ratio of the invisible decay $\tilde{\chi}_1^0 \to 3\,\nu$. This branching ratio can reach 7% for the parameters chosen. In Figs. 7 and 8 we show the branching ratio for the decays $\tilde{\chi}_1^0 \to \nu_3 l^+ l^-$ and $\tilde{\chi}_1^0 \to \nu_3 q\bar{q}$ where l and q denote the leptons and quarks of the first two generations, summed over all flavors. These branching ratios can go up to 3% and 15%, respectively. Notice that the sneutrino, slepton, and squark exchange contributions to the $\tilde{\chi}_1^0$ decays become larger with increasing m_0, despite the fact that the increase of the scalar masses $m_{\tilde{\nu}}$, $m_{\tilde{l}}$, $m_{\tilde{q}}$ suppresses these exchange contributions. This trend can also be observed in Figs. 8, 9 and 10. This happens because the tadpole equations correlate μ to m_0. Increasing μ while keeping M_1 and M_2 fixed implies increasing the gaugino content of $\tilde{\chi}_1^0$ and, hence, enhancing the $\tilde{\chi}_1^0 - f - \tilde{f}$ couplings.

In Figs. 9 and 10 we show the contour lines for the branching ratios of the LSP decays involving a single tau, namely, $\tilde{\chi}_1^0 \to \nu_l \tau^{\pm} l^{\mp}$ and $\tilde{\chi}_1^0 \to \tau^{\pm} q\bar{q}'$, where l, q, and q' are summed over the first two generations. The branching for these decay modes can reach up to 20% and 60%, respectively. For $M_{1/2} \gtrsim 220$ GeV decays into real $W^{\pm}$ dominate. If this is the case and if both $\tilde{\chi}_1^0$ produced in $e^+e^- \to \tilde{\chi}_1^0\tilde{\chi}_1^0$ decay according to these modes this would lead to very distinctive final states, such as $4j\tau^+\tau^+$, $\tau^+\tau^+l^-l^-$ ($l = e, \mu$), or $\tau^+\tau^+e^-\mu^-$. The full list of expected signals is given in Table 2. The first column in this table specifies the two pairs of $\tilde{\chi}_1^0$ decay modes, while the second one gives the corresponding signature. In the last column we state whether the corresponding signature exists for $e^+e^- \to \tilde{\chi}_1^0\tilde{\chi}_2^0$ production within mSUGRA.

The LSP decays involving only third generation fermions, namely, $\tilde{\chi}_1^0 \to \nu_3 b\bar{b}$ and $\tilde{\chi}_1^0 \to \nu_3\,\tau^+\tau^-$ are different from those into the first and second generation fermion pairs, because the Higgs boson exchanges and the Yukawa terms play a very important rôle. This can be seen in Figs. 11 and 12, where we plot the contour lines for these decays. The branching ratio of $\tilde{\chi}_1^0 \to \nu_3 b\bar{b}$ can reach up to 97%. The decay rate is large because the scalar exchange contributions (S_j^0, P_j^0, $\tilde{b}_k$) are large for $M_{1/2} \lesssim 200$ GeV. Note that this is also the case for $\tan\beta = 3$, because not only the neutrino–neutralino mixing proportional to m_{ν_3} is important but also the neutrino–higgsino mixing proportional to ϵ_3/μ. The decrease of the branching ratio with increasing m_0 is due to the decrease of the higgsino component of $\tilde{\chi}_1^0$ and the increase of the Higgs boson masses. For $M_{1/2} \gtrsim 200$ GeV the decays into real W^+ and Z^0 are possible, reducing the branching ratio of $\tilde{\chi}_1^0 \to \nu_3 b\bar{b}$. As shown in Fig. 12

Table 2
The signatures expected from the process $e^+e^- \to \tilde{\chi}_1^0\tilde{\chi}_1^0$ in the bilinear $\not{R}_p$ model

Combination of $\tilde{\chi}_1^0$ decay modes	Signature	mSUGRA-like
$(3\,\nu)$ $(3\,\nu)$	$\not{p}_T$	yes
$(3\,\nu)$ $(\nu_3 l^+ l^-)$	2 leptons $+ \not{p}_T$	yes
$(3\,\nu)$ $(\nu_3 q\bar{q})$	2 jets $+ \not{p}_T$	yes
$(3\,\nu)$ $(\nu_3 b\bar{b})$		
$(3\,\nu)$ $(\nu_l \tau^\pm l^\mp)$ with $l = e, \mu$	$\tau + (e$ or $\mu) + \not{p}_T$	yes, but suppressed
$(3\,\nu)$ $(\tau^\pm q\bar{q}')$	$\tau + 2$ jets $+ \not{p}_T$	yes, but suppressed
$(3\,\nu)$ $(\nu_3\,\gamma)$	$\gamma + \not{p}_T$	yes
$(\nu_3 l^+ l^-)$ $(\nu_3 l'^+ l'^-)$	4 leptons $+ \not{p}_T$	no
$(\nu_3 l^+ l^-)$ $(\nu_3 q\bar{q})$	2 leptons $+ 2$ jets $+ \not{p}_T$	no
$(\nu_3 l^+ l^-)$ $(\nu_3 b\bar{b})$		
$(\nu_3 l^+ l^-)$ $(\nu_l \tau^\pm l^\mp)$ with $l = e, \mu$	$\tau + 3$ (e and/or $\mu) + \not{p}_T$	no
$(\nu_3 \tau^+ \tau^-)$ $(\nu_l \tau^\pm l^\mp)$ with $l = e, \mu$	$3\,\tau + (e$ or $\mu) + \not{p}_T$	no
$(\nu_3 l^+ l^-)$ $(\tau^\pm q\bar{q}')$	$\tau + 2$ leptons $+ 2$ jets $+ \not{p}_T$	no
$(\nu_3 \tau^+ \tau^-)$ $(\tau^\pm q\bar{q}')$	$3\,\tau + 2$ jets $+ \not{p}_T$	no
$(\nu_3 l^+ l^-)$ $(\nu_3 \gamma)$	2 leptons $+ \gamma + \not{p}_T$	no
$(\nu_3 q\bar{q})$ $(\nu_3 q\bar{q})$	4 jets $+ \not{p}_T$	yes, but suppressed
$(\nu_3 q\bar{q})$ $(\nu_3 b\bar{b})$		
$(\nu_3 b\bar{b})$ $(\nu_3 b\bar{b})$		
$(\nu_3 q\bar{q})$ $(\nu_l \tau^\pm l^\mp)$ with $l = e, \mu$	$\tau + (e$ or $\mu) + 2$ jets $+ \not{p}_T$	no
$(\nu_3 b\bar{b})$ $(\nu_l \tau^\pm l^\mp)$ with $l = e, \mu$		
$(\nu_3 q\bar{q})$ $(\tau^\pm q\bar{q}')$	$\tau + 4$ jets $+ \not{p}_T$	no
$(\nu_3 b\bar{b})$ $(\tau^\pm q\bar{q}')$		
$(\nu_3 q\bar{q})$ $(\nu_3 \gamma)$	2 jets $+ \gamma + \not{p}_T$	no
$(\nu_3 b\bar{b})$ $(\nu_3 \gamma)$		
$(\nu_l \tau^\pm l^\mp)$ $(\nu_l \tau^\pm l'^\mp)$	$\tau^\pm\tau^\pm + l^\mp l'^\mp + \not{p}_T$	no
	$\tau^\pm\tau^\mp + l^\mp l'^\pm + \not{p}_T$	no
$(\nu_l \tau^\pm l^\mp)$ $(\tau^\pm q\bar{q}')$	$\tau^\pm\tau^\pm + (e$ or $\mu) + 2$ jets $+ \not{p}_T$	no
	$\tau^\pm\tau^\mp + (e$ or $\mu) + 2$ jets $+ \not{p}_T$	no
$(\nu_l \tau^\pm l^\mp)$ $(\nu_3 \gamma)$	$\tau + (e$ or $\mu) + \gamma + \not{p}_T$	no
$(\tau^\pm q\bar{q}')$ $(\tau^\pm q\bar{q}')$	$\tau^\pm\tau^\pm + 4$ jets $+ \not{p}_T$	no
	$\tau^\pm\tau^\mp + 4$ jets $+ \not{p}_T$	no
$(\tau^\pm q\bar{q}')$ $(\nu_3 \gamma)$	$\tau + 2$ jets $+ \gamma + \not{p}_T$	no
$(\nu_3 \gamma)$ $(\nu_3 \gamma)$	$2\,\gamma + \not{p}_T$	no

the branching ratio for $\tilde{\chi}_1^0 \to \nu_3 \tau^+ \tau^-$ is very small for $\tan\beta = 3$ and $M_{1/2} \lesssim 200$ GeV. This is due to the destructive interference between Z^0 contribution and the contributions of the exchanged charged scalar particles (mainly due to the stau components of $S_k^\pm$).

Finally, we have also considered the radiative LSP decay mode $\tilde{\chi}_1^0 \to \nu_3 \gamma$ [29]. In Fig. 13 the branching ratio for this mode is shown. This decay proceeds only at one-loop level and therefore is in general suppressed compared to the three-body decay modes. However, for $M_{1/2} \lesssim 125$ GeV and large $\tan\beta$ it exceeds 1%, leading to interesting signatures like $e^+e^- \to \tilde{\chi}_1^0 \tilde{\chi}_1^0 \to \tau^\pm \mu^\mp \gamma + \not{p}_T$. Due to initial state radiation it can easily happen that a second photon is observed in the same event.

The complete list of possible signatures stemming from LSP decays in our bilinear $\not{R}_p$ model is shown in Table 2. In this table we also indicate whether the same signatures could also arise in mSUGRA as a result of $e^+e^- \to \tilde{\chi}_1^0 \tilde{\chi}_2^0$ followed by the MSSM decay modes of $\tilde{\chi}_2^0$ if its production is kinematically allowed. The final states 4 jets $+ \not{p}_T$, $\tau + 2$ jets $+ \not{p}_T$, and $\tau + (e$ or $\mu) + \not{p}_T$ would also occur in mSUGRA via the decay of $\tilde{\chi}_2^0$ into $\tilde{\chi}_1^\pm$. However, one expects in general that these decay modes are suppressed within mSUGRA. In contrast in the R-parity violating case these signatures can be rather large as can be seen from Figs. 9 and 10. Note moreover, that some of the $\not{R}_p$ signatures are practically background free. For example, due to the Majorana nature of $\tilde{\chi}_1^0$, one can have two same-sign τ leptons + 4 jets + $\not{p}_T$. Other interesting signals are: $\tau + 3$ (e and/or μ) + $\not{p}_T$, $3\tau + (e$ or $\mu) + \not{p}_T$, $\tau + (e$ or $\mu) + 2$ jets + $\not{p}_T$, $\tau + 4$ jets + $\not{p}_T$, $\tau^\pm \tau^\pm + (e$ or $\mu) +$ 2 jets + $\not{p}_T$, or $\tau^\pm \tau^\pm + l^\mp l'^\mp + \not{p}_T$ with $l = e, \mu$. In Table 3 we give masses and branching ratios for typical examples.

As it is well known, also in gauge mediated supersymmetry breaking models (GMSB) [18] the neutralino can decay inside the detector, because the gravitino $\widetilde{G}$ is the LSP. It is, therefore, an interesting question if the R-parity violating model can be confused with GMSB. To answer this question let us have a look at the dominant decay modes of the lightest neutralino in GMSB. If the lightest neutralino is the NLSP, its main decay mode in GMSB is

$$\tilde{\chi}_1^0 \to \gamma \widetilde{G},$$

where $\widetilde{G}$ is the gravitino. For the case where at least one of the sleptons is lighter than the lightest neutralino the latter has the following decay chain $\tilde{\chi}_1^0 \to \tilde{l}^\pm l^\mp \to l^\pm l^\mp \widetilde{G}$. In principle three-body decay modes mediated by virtual photon, virtual Z-boson and virtual sfermions also exist. However, in the neutralino mass range considered here these decays are phase–space-suppressed [18,30]. This implies that the R-parity violating model cannot be confused with GMSB, because (i) in GMSB the final states containing quarks are strongly suppressed, and (ii) GMSB with conserved R-parity implies lepton flavour conservation, and, therefore, there are no final states like $e^+e^+\tau^-\tau^- + \not{p}_T$. A further interesting question would be how the neutralino phenomenology changes in a GMSB scenario with broken R-parity. The main consequence would be an enhancement of final states containing photons and/or leptons. A detailed study of this question is, however, beyond the scope of the present paper.

Table 3
Masses and branching ratios for the points: A $(M_{1/2}, m_0) = (153, 155)$, B $(M_{1/2}, m_0) = (153, 440)$, and C $(M_{1/2}, m_0) = (251, 440)$ for both $\tan\beta = 3$ and 50. The masses are given in GeV and the branching ratios in % and we only give those larger than 0.1%. Here the same summations of the final states are performed as in the figures. $m_{\tilde{q}}$ is the averaged squark mass for the first two generations

	$\tan\beta = 3$			$\tan\beta = 50$		
	A	B	C	A	B	C
$m_{\tilde{\chi}_1^0}$	54.6	59.0	92.5	60.0	61.5	94.4
$m_{S_1^0}$	91.0	96.8	102.9	107.2	111.1	116.4
$m_{\tilde{\nu}}$	180.5	449.6	466.0	178.2	448.7	465.1
$m_{\tilde{e}_R}$	170.5	445.7	450.6	171.6	446.1	451.0
$m_{\tilde{e}_L}$	194.2	455.2	471.4	195.3	455.8	471.9
$m_{\tilde{q}}$	398.1	572.8	705.4	398.1	572.8	705.4
$m_{\tilde{t}_1}$	261.4	328.5	442.2	279.9	355.2	466.3
$m_{\tilde{b}_1}$	361.3	479.1	612.1	243.0	343.0	470.1
$\mathrm{BR}(\tilde{\chi}_1^0 \to 3\nu)$	0.5	4.5	1.8	0.3	1.2	1.9
$\mathrm{BR}(\tilde{\chi}_1^0 \to l^- l^+ \nu_3)$	0.2	1.1	0.5	0.2	0.3	0.6
$\mathrm{BR}(\tilde{\chi}_1^0 \to q\bar{q}\nu_3)$	1.0	8.6	4.0	0.5	2.2	4.4
$\mathrm{BR}(\tilde{\chi}_1^0 \to l^\pm \tau^\mp \nu)$	0.6	5.6	18.0	0.5	1.8	17.8
$\mathrm{BR}(\tilde{\chi}_1^0 \to q\bar{q}'\tau^\pm)$	1.1	16.1	53.7	0.9	5.1	53.2
$\mathrm{BR}(\tilde{\chi}_1^0 \to b\bar{b}\nu_3)$	96.5	62.6	13.4	97.1	88.4	13.3
$\mathrm{BR}(\tilde{\chi}_1^0 \to \tau^-\tau^+\nu_3)$	0.1	1.5	8.6	0.5	1.0	8.8

4. Conclusions

We have studied the production of the lightest neutralino $\tilde{\chi}_1^0$ at LEP2 and the resulting phenomenology in models where an effective bilinear term in the superpotential parametrizes the explicit breaking of R-parity. We have considered supergravity scenarios which can be explored at LEP2 in which the lightest neutralino is also the lightest supersymmetric particle. We have presented a detailed study of the LSP $\tilde{\chi}_1^0$ decay properties and studied the general features of the corresponding signals expected at LEP2. A detailed investigation of the possible detectability of the signals discussed in Table 2 taking into account realistic detector features is beyond the scope of this paper. Clearly, existing LEP2 data are already probing the part of the parameter region which corresponds to approximately $m_{\tilde{\chi}_1^0} \lesssim 40$ GeV. Finally, we note that, in addition to important modifications in the $\tilde{\chi}_1^0$ decay properties, R-parity violating decay models lead also to new interesting features in other decays, such as charged [21] and neutral [28] Higgs boson and slepton decays, stop decays [22,31,32], and gluino cascade decays [33]. In addition we have shown that the R-parity violating model cannot be confused with gauge mediated supersymmetry breaking and conserved R-parity due to the absence of several final states in the GMSB case.

Acknowledgements

This work was supported by "Fonds zur Förderung der wissenschaftlichen Forschung" of Austria, project No. P13139-PHY, by Spanish DGICYT grants PB98-0693 and by the EEC under the TMR contract HPRN-CT-2000-00148. W.P. was supported by a fellowship from the Spanish Ministry of Culture under the contract SB97-BU0475382. D.R. was supported by Colombian COLCIENCIAS fellowship.

Appendix A. Scalar mass matrices

The mass matrix of the charged scalar sector follows from the quadratic terms in the scalar potential [21,22].

$$V_{\text{quadratic}} = \mathbf{S}'^{-}\mathbf{M}^2_{\mathrm{S}^\pm}\mathbf{S}'^{+}, \tag{A.1}$$

where $\mathbf{S}'^{-} = [\mathbf{H}_1^-, \mathbf{H}_2^-, \tilde{\tau}_{\mathrm{L}}^-, \tilde{\tau}_{\mathrm{R}}^-]$. For convenience reasons we will divide this 4×4 matrix into 2×2 blocks in the following way:

$$\mathbf{M}^2_{\mathrm{S}^\pm} = \begin{bmatrix} \mathbf{M}^2_{\mathrm{HH}} & \mathbf{M}^{2\,\mathbf{T}}_{\mathrm{H}\tilde{\tau}} \\ \mathbf{M}^2_{\mathrm{H}\tilde{\tau}} & \mathbf{M}^2_{\tilde{\tau}\tilde{\tau}} \end{bmatrix}, \tag{A.2}$$

where the charged Higgs block is

$$\mathbf{M}^2_{\mathrm{HH}} = \begin{bmatrix} B\mu\frac{v_2}{v_1} + \frac{1}{4}g^2\left(v_2^2 - v_3^2\right) + \mu\epsilon_3\frac{v_3}{v_1} + \frac{1}{2}h_\tau^2 v_3^2 + \frac{t_1}{v_1} & B\mu + \frac{1}{4}g^2 v_1 v_2 \\ B\mu + \frac{1}{4}g^2 v_1 v_2 & B\mu\frac{v_1}{v_2} + \frac{1}{4}g^2\left(v_1^2 + v_3^2\right) - B_3\epsilon_3\frac{v_3}{v_2} + \frac{t_2}{v_2} \end{bmatrix}, \tag{A.3}$$

and h_τ is the tau Yukawa coupling.

$$\mathbf{M}^2_{\tilde{\tau}\tilde{\tau}} = \begin{bmatrix} \frac{1}{2}h_\tau^2 v_1^2 - \frac{1}{4}g^2\left(v_1^2 - v_2^2\right) + \mu\epsilon_3\frac{v_1}{v_3} - B_3\epsilon_3\frac{v_2}{v_3} + \frac{t_3}{v_3} & \frac{1}{\sqrt{2}}h_\tau(A_\tau v_1 - \mu v_2) \\ \frac{1}{\sqrt{2}}h_\tau(A_\tau v_1 - \mu v_2) & m^2_{R_3} + \frac{1}{2}h_\tau^2\left(v_1^2 + v_3^2\right) - \frac{1}{4}g'^2\left(v_1^2 - v_2^2 + v_3^2\right) \end{bmatrix}. \tag{A.4}$$

The mixing between the charged Higgs sector and the stau sector is given by the following 2×2 block:

$$\mathbf{M}^2_{\mathrm{H}\tilde{\tau}} = \begin{bmatrix} -\mu\epsilon_3 - \frac{1}{2}h_\tau^2 v_1 v_3 + \frac{1}{4}g^2 v_1 v_3 & -B_3\epsilon_3 + \frac{1}{4}g^2 v_2 v_3 \\ -\frac{1}{\sqrt{2}}h_\tau(\epsilon_3 v_2 + A_\tau v_3) & -\frac{1}{\sqrt{2}}h_\tau(\mu v_3 + \epsilon_3 v_1) \end{bmatrix}. \tag{A.5}$$

As we see the charged Higgs bosons mix with charged sleptons.

In a similar way the real (imaginary) parts of the sneutrino mix the scalar (pseudoscalar) Higgs bosons. The quadratic scalar potential responsible for the neutral Higgs sector mass matrices includes

$$V_{\text{quadratic}} = \frac{1}{2}\left(\mathbf{P}'^0\right)^{\mathrm{T}}\mathbf{M}^2_{\mathrm{P}^0}\mathbf{P}'^0 + \left(\mathbf{S}'^0\right)^{\mathrm{T}}\mathbf{M}^2_{\mathrm{S}^0}\mathbf{S}'^0 + \cdots, \tag{A.6}$$

where $(\mathbf{P}'^0)^{\mathrm{T}} = [\varphi_1^0, \varphi_2^0, \tilde{\nu}_\tau^{\mathrm{I}}]$, $(\mathbf{S}'^0)^{\mathrm{T}} = \frac{1}{2}[\chi_1^0, \chi_2^0, \tilde{\nu}_\tau^{\mathrm{R}}]$ and the CP-odd neutral scalar mass matrix is

$$\mathbf{M}^2_{\mathrm{P}^0} = \begin{bmatrix} B\mu\frac{v_2}{v_1} + \mu\epsilon_3\frac{v_3}{v_1} + \frac{t_1}{v_1} & B\mu & -\mu\epsilon_3 \\ B\mu & B\mu\frac{v_1}{v_2} - B_3\epsilon_3\frac{v_3}{v_2} + \frac{t_2}{v_2} & -B_3\epsilon_3 \\ -\mu\epsilon_3 & -B_3\epsilon_3 & \mu\epsilon_3\frac{v_1}{v_3} - B_3\epsilon_3\frac{v_2}{v_3} + \frac{t_3}{v_3} \end{bmatrix}. \tag{A.7}$$

The neutral CP-even scalar sector mass matrix in Eq. (A.6) is given by

$$\mathbf{M}^2_{\mathrm{S}^0} = \begin{bmatrix} B\mu\frac{v_2}{v_1} + \frac{1}{4}g_Z^2 v_1^2 + \mu\epsilon_3\frac{v_3}{v_1} + \frac{t_1}{v_1} & -B\mu - \frac{1}{4}g_Z^2 v_1 v_2 & -\mu\epsilon_3 + \frac{1}{4}g_Z^2 v_1 v_3 \\ -B\mu - \frac{1}{4}g_Z^2 v_1 v_2 & B\mu\frac{v_1}{v_2} + \frac{1}{4}g_Z^2 v_2^2 - B_3\epsilon_3\frac{v_3}{v_2} + \frac{t_2}{v_2} & B_3\epsilon_3 - \frac{1}{4}g_Z^2 v_2 v_3 \\ -\mu\epsilon_3 + \frac{1}{4}g_Z^2 v_1 v_3 & B_3\epsilon_3 - \frac{1}{4}g_Z^2 v_2 v_3 & \mu\epsilon_3\frac{v_1}{v_3} - B_3\epsilon_3\frac{v_2}{v_3} + \frac{1}{4}g_Z^2 v_3^2 + \frac{t_3}{v_3} \end{bmatrix}, \tag{A.8}$$

where we have defined $g_Z^2 \equiv g^2 + g'^2$. Note that, as a result of CP invariance, the CP-even and CP-odd parts of the scalar mass matrices are disjoint and do not mix with each other.

The three mass matrices in Eqs. (A.2), (A.7), and (A.8) are diagonalized by rotation matrices which define the eigenvectors

$$\mathbf{S}^+ = \mathbf{R}_{\mathrm{S}^\pm}\mathbf{S}'^+, \qquad \mathbf{P}^0 = \mathbf{R}_{\mathrm{P}^0}\mathbf{P}'^0, \qquad \mathbf{S}^0 = \mathbf{R}_{\mathrm{S}^0}\mathbf{S}'^0, \tag{A.9}$$

and the eigenvalues

$$\begin{aligned} &\mathrm{diag}\Big(0, m^2_{\mathrm{S}^\pm_2}, m^2_{\mathrm{S}^\pm_3}, m^2_{\mathrm{S}^\pm_4}\Big) = \mathbf{R}_{\mathrm{S}^\pm}\mathbf{M}^2_{\mathrm{S}^\pm}\mathbf{R}^{\mathrm{T}}_{\mathrm{S}^\pm} \quad \text{for the charged scalars,} \\ &\mathrm{diag}\Big(0, m^2_{\mathrm{P}^0_2}, m^2_{\mathrm{P}^0_3}\Big) = \mathbf{R}_{\mathrm{P}^0}\mathbf{M}^2_{\mathrm{P}^0}\mathbf{R}^{\mathrm{T}}_{\mathrm{P}^0} \quad \text{for the CP-odd neutral scalars,} \\ &\mathrm{diag}\Big(m^2_{\mathrm{S}^0_1}, m^2_{\mathrm{S}^0_2}, m^2_{\mathrm{S}^0_3}\Big) = \mathbf{R}_{\mathrm{S}^0}\mathbf{M}^2_{\mathrm{S}^0}\mathbf{R}^{\mathrm{T}}_{\mathrm{S}^0} \quad \text{for the CP-even neutral scalars.} \end{aligned}$$

The matrices $\mathbf{R}_{\mathrm{S}^\pm}$, $\mathbf{R}_{\mathrm{P}^0}$ and $\mathbf{R}_{\mathrm{S}^0}$ specify the mixing between the Higgs sector and the stau sector.

If a 3×3 matrix $\mathbf{M}$ has a zero eigenvalue, then the other two eigenvalues satisfy

$$\begin{aligned} m_\pm = {} & \frac{1}{2}\,\mathrm{Tr}\,\mathbf{M} \\ & \pm \frac{1}{2}\sqrt{(\mathrm{Tr}\,\mathbf{M})^2 - 4(\mathbf{M}_{11}\mathbf{M}_{22} - \mathbf{M}^2_{12} + \mathbf{M}_{11}\mathbf{M}_{33} - \mathbf{M}^2_{13} + \mathbf{M}_{22}\mathbf{M}_{33} - \mathbf{M}^2_{23})}. \end{aligned} \tag{A.10}$$

The CP-odd neutral scalar mass matrix Eq. (A.7) has a zero determinant, so that its eigenvalues $m^2_{\mathrm{P}^0_2}$ and $m^2_{\mathrm{P}^0_3}$ (m_A^2 and $m^2_{\tilde{\nu}_\tau^R}$ in the MSSM limit) can be calculated exactly with the previous formula.

References

[1] G. Altarelli, T. Sjöstrand, F. Zwirner (Eds.), Proc. of the Workshop on Physics at LEP2, CERN 96-01, Vol. 1, 1996, p. 463, hep-ph/9602207;

J. Amundson et al., in: D.G. Cassel, L. Trindle Gennari, R.H. Siemann (Eds.), Proceedings of the 1996 DPF/DPB Summer Study on High-Energy Physics, Snowmass, Colorado, 1996, p. 655;
A. Bartl et al., in: D.G. Cassel, L. Trindle Gennari, R.H. Siemann (Eds.), Proceedings of the 1996 DPF/DPB Summer Study on High-Energy Physics, Snowmass, Colorado, 1996, p. 693;
S. Mrenna et al., in: D.G. Cassel, L. Trindle Gennari, R.H. Siemann (Eds.), Proceedings of the 1996 DPF/DPB Summer Study on High-Energy Physics, Snowmass, Colorado, 1996, p. 681;
M. Carena et al., hep-ex/9802006;
M. Carena et al., hep-ex/9712022;
ECFA/DESY LC Physics Working Group, E. Accomando et al., Phys. Rep. 299 (1998) 1.

[2] The global MSW discussion of the solar neutrino data is given in: M.C. Gonzalez-Garcia, P.C. de Holanda, C. Peña-Garay, J.W.F. Valle, Nucl. Phys. B 573 (2000) 3, hep-ph/9906469;
For prospects see J.N. Bahcall, P.I. Krastev, A.Y. Smirnov, hep-ph/0002293;
G.L. Fogli, E. Lisi, D. Montanino, A. Palazzo, Phys. Rev. D 61 (2000) 073009;
For an update see M.C. Gonzalez-Garcia et al., Global three-neutrino oscillation analysis of neutrino data, hep-ph/0009350, Phys. Rev. D 63 (2001) 033005.

[3] For recent global fits of atmospheric neutrino data see, for example, N. Fornengo, M.C. Gonzalez-Garcia, J.W.F. Valle, Nucl. Phys. B 580 (2000) 58, hep-ph/0002147;
M.C. Gonzalez-Garcia, H. Nunokawa, O.L. Peres, J.W.F. Valle, Nucl. Phys. B 543 (1999) 3;
G.L. Fogli, E. Lisi, A. Marrone, G. Scioscia, Combined analysis of atmospheric neutrino results, in: Venice 1999, Neutrino Telescopes, Vol. 1, 1999, pp. 275–282;
R. Foot, R.R. Volkas, O. Yasuda, Phys. Rev. D 58 (1998) 013006;
For an update see: M.C. Gonzalez-Garcia et al., Global three-neutrino oscillation analysis of neutrino data, hep-ph/0009350, Phys. Rev. D 63 (2001) 033005.

[4] For recent papers see, for example, J.C. Romão, M.A. Díaz, M. Hirsch, W. Porod, J.W.F. Valle, Phys. Rev. D 61 (2000) 071703, hep-ph/9907499;
For a more extensive study see M. Hirsch, M.A. Díaz, W. Porod, J.C. Romão, J.W.F. Valle, Phys. Rev. D 62 (2000) 113008, hep-ph/0004115.
These papers give a fair reference list on this subject.

[5] L. Hall, M. Suzuki, Nucl. Phys. B 231 (1984) 419;
S. Dimopoulos, L.J. Hall, Phys. Lett. B 207 (1988) 210;
E. Ma, D. Ng, Phys. Rev. D 41 (1990) 1005;
V. Barger, G.F. Giudice, T. Han, Phys. Rev. D 40 (1989) 2987;
T. Banks, Y. Grossman, E. Nardi, Y. Nir, Phys. Rev. D 52 (1995) 5319;
M. Nowakowski, A. Pilaftsis, Nucl. Phys. B 461 (1996) 19;
G. Bhattacharyya, D. Choudhury, K. Sridhar, Phys. Lett. B 349 (1995) 118;
B. de Carlos, P.L. White, Phys. Rev. D 54 (1996) 3427.

[6] C.S. Aulakh, R.N. Mohapatra, Phys. Lett. B 119 (1982) 116;
G.G. Ross, J.W.F. Valle, Phys. Lett. B 151 (1985) 375;
J. Ellis, G. Gelmini, C. Jarlskog, G.G. Ross, J.W.F. Valle, Phys. Lett. B 150 (1985) 142.

[7] A. Santamaria, J.W.F. Valle, Phys. Lett. B 195 (1987) 423;
A. Santamaria, J.W.F. Valle, Phys. Rev. D 39 (1989) 1780;
A. Santamaria, J.W.F. Valle, Phys. Rev. Lett. 60 (1988) 397.

[8] See, e.g., J.W.F. Valle, in: Physics Beyond the Standard Model, lectures given at the VIII Jorge Andre Swieca Summer School, Rio de Janeiro, February 1995, and at V Taller Latinoamericano de Fenomenologia de las Interacciones Fundamentales, Puebla, Mexico, October 1995, hep-ph/9603307.

[9] J.W.F. Valle, Phys. Lett. B 196 (1987) 157;
M.C. Gonzalez-García, J.W.F. Valle, Nucl. Phys. B 355 (1991) 330;
K. Huitu, J. Maalampi, Phys. Lett. B 344 (1995) 217, hep-ph/9410342.

[10] A. Masiero, J.W.F. Valle, Phys. Lett. B 251 (1990) 273;

J.C. Romão, C.A. Santos, J.W.F. Valle, Phys. Lett. B 288 (1992) 311;
J.C. Romão, A. Ioannisian, J.W.F. Valle, Phys. Rev. D 55 (1997) 427, hep-ph/9607401.
[11] G. Giudice, A. Masiero, M. Pietroni, A. Riotto, Nucl. Phys. B 396 (1993) 243;
M. Shiraishi, I. Umemura, K. Yamamoto, Phys. Lett. B 313 (1993) 89;
See also: I. Umemura, K. Yamamoto, Nucl. Phys. B 423 (1994) 405.
[12] For recent reviews see: J.W.F. Valle, in: P. Nath (Ed.), Supergravity Unification with Bilinear R-Parity Violation, Proceedings of PASCOS98, World Scientific, 1998, hep-ph/9808292;
J.C. Romão, M. Díaz, in: Proceedings of the 4th Bi-Annual Meeting: Frontiers in High Energy and Astroparticle Physics, Beyond the Standard Model: From Theory to Experiment, Valencia, Spain, October 13–17, 1997, World Scientific, 1998.
[13] P. Nogueira, J.C. Romão, J.W.F. Valle, Phys. Lett. B 251 (1990) 142;
R. Barbieri, L. Hall, Phys. Lett. B 238 (1990) 86;
M.C. Gonzalez-Garcia, J.W.F. Valle, Nucl. Phys. B 355 (1991) 330;
M.C. Gonzalez-Garcia, J.C. Romão, J.W.F. Valle, Nucl. Phys. B 391 (1993) 100;
For an updated description see: A.G. Akeroyd, M.A. Díaz, J.W.F. Valle, Phys. Lett. B 441 (1998) 224, hep-ph/9806382.
[14] L. Navarro, W. Porod, J.W.F. Valle, Phys. Lett. B 459 (1999) 615, hep-ph/9903474.
[15] B. Mukhopadhyaya, S. Roy, F. Vissani, Phys. Lett. B 443 (1998) 191, hep-ph/9808265;
S.Y. Choi, E.J. Chun, S.K. Kang, J.S. Lee, Phys. Rev. D 60 (1999) 075002, hep-ph/9903465.
[16] F. de Campos, O.J. Eboli, M.A. Garcia-Jareño, J.W.F. Valle, Nucl. Phys. B 546 (1999) 33, hep-ph/9710545.
[17] M.A. Díaz, J.C. Romão, J.W.F. Valle, Nucl. Phys. B 524 (1998) 23–40, hep-ph/9706315;
M.A. Díaz, J. Ferrandis, J.C. Romão, J.W.F. Valle, Phys. Lett. B 453 (1999) 263, hep-ph/9801391;
M.A. Díaz, J. Ferrandis, J.C. Romão, J.W.F. Valle, hep-ph/9906343;
M.A. Díaz, J. Ferrandis, J.W.F. Valle, Nucl. Phys. B 573 (2000) 75, hep-ph/9909212.
[18] For a general review see of GMSB, G.F. Giudice, R. Rattazzi, Phys. Rep. 322 (1999) 419.
[19] The signals relevant for LEP2 are discussed, e.g., in: S. Ambrosanio, B. Mele, Phys. Rev. D 52 (1995) 3900.
[20] S. Roy, B. Mukhopadhyaya, Phys. Rev. D 55 (1997) 7020, hep-ph/9903418;
A. Datta, B. Mukhopadhyaya, S. Roy, Phys. Rev. D 61 (2000) 055006, hep-ph/9905549;
T. Feng, hep-ph/980650, hep-ph/9808379;
C. Chang, T. Feng, Eur. Phys. J. C 12 (2000) 137, hep-ph/9901260.
[21] A. Akeroyd, M.A. Díaz, J. Ferrandis, M.A. Garcia-Jareño, J.W.F. Valle, Nucl. Phys. B 529 (1998) 3.
[22] W. Porod, D. Restrepo, J.W.F. Valle, hep-ph/0001033, LC-TH-2000-005.
[23] M.A. Díaz, E. Torrente-Lujan, J.W.F. Valle, Nucl. Phys. B 551 (1999) 78, hep-ph/9808412.
[24] J.C. Romão, J.W.F. Valle, Phys. Lett. B 272 (1991) 436;
J.C. Romão, J.W.F. Valle, Nucl. Phys. B 381 (1992) 87.
[25] A. Bartl, H. Fraas, W. Majerotto, Nucl. Phys. B 278 (1986) 1.
[26] E.A. Kuraev, V.S. Fadin, Sov. J. Nucl. Phys. 41 (1985) 3;
M.E. Peskin, in: Physics at the 100 GeV Mass Scale, 17th SLAC Summer Institute, 1989.
[27] A. Bartl, W. Majerotto, W. Porod, Phys. Lett. B 465 (1999) 187.
[28] F. de Campos, M.A. Garcia-Jareño, A.S. Joshipura, J. Rosiek, J.W.F. Valle, Nucl. Phys. B 451 (1995) 3, hep-ph/9502237.
[29] B. Mukhopadhyaya, S. Roy, Phys. Rev. D 60 (1999) 115012, hep-ph/9903418.
[30] J.A. Bagger, K. Matchev, D.M. Pierce, R. Zhang, Phys. Rev. D 55 (1997) 3188, hep-ph/9609444.
[31] A. Bartl, W. Porod, M.A. Garcia-Jareño, M.B. Magro, J.W.F. Valle, W. Majerotto, Phys. Lett. B 384 (1996) 151.
[32] M.A. Díaz, D.A. Restrepo, J.W.F. Valle, Nucl. Phys. B 583 (2000) 182, hep-ph/9908286.

[33] H. Dreiner, G.G. Ross, Nucl. Phys. B 365 (1991) 597;
H. Dreiner, M. Guachit, D.P. Roy, Phys. Rev. D 49 (1994) 3270;
A. Bartl, W. Majerotto, W. Porod, Z. Phys. C 64 (1994) 499;
A. Bartl, W. Majerotto, W. Porod, Z. Phys. C 68 (1995) 515, Erratum;
A. Bartl et al., Nucl. Phys. B 502 (1997) 19;
A. Bartl et al., in: I. Antoniadis, L.E. Ibáñez, J.W.F. Valle (Eds.), Proceedings of the International Workshop on Physics Beyond the Standard Model: From Theory to Experiment, Valencia, Spain, 13–17 October, 1997, pp. 200–204, hep-ph/9712484.